THE JOURNAL OF BIOLOGICAL CHEMISTRY VOL. 290, NO. 32, pp. 19874–19887, August 7, 2015


# Yeast Fex1p Is a Constitutively Expressed Fluoride Channel with Functional Asymmetry of Its Two Homologous Domains*[S]

Received for publication, March 13, 2015, and in revised form, June 3, 2015 Published, JBC Papers in Press, June 8, 2015, DOI 10.1074/jbc.M115.651976

**Kathryn D. Smith[‡], Patricia B. Gordon[‡], Alberto Rivetta[§], Kenneth E. Allen[¶], Tetyana Berbasova[‡], Clifford Slayman[§], and Scott A. Strobel[‡‖1]**

*From the Departments of [‡]Molecular Biophysics and Biochemistry, [§]Cellular and Molecular Physiology, [¶]Genetics, and [‖]Chemistry, Yale University, New Haven, Connecticut 06520*

**Background:** Fluoride is broadly toxic, and organisms use fluoride export (FEX) proteins to expel it.
**Results:** FEX is a constitutively expressed fluoride channel, and mutations to the C- and N-terminal domains have asymmetric effects.
**Conclusion:** Protection from fluoride is constantly needed, and a positive residue in the membrane is required.
**Significance:** Understanding FEX furthers our knowledge of fluoride resistance mechanisms.

**Fluoride is a ubiquitous environmental toxin with which all biological species must cope. A recently discovered family of fluoride export (FEX) proteins protects organisms from fluoride toxicity by removing it from the cell. We show here that FEX proteins in *Saccharomyces cerevisiae* function as ion channels that are selective for fluoride over chloride and that these proteins are constitutively expressed at the yeast plasma membrane. Continuous expression is in contrast to many other toxin exporters in yeast, and this, along with the fact that two nearly duplicate proteins are encoded in the yeast genome, suggests that the threat posed by fluoride ions is frequent and detrimental. Structurally, eukaryotic FEX proteins consist of two homologous four-transmembrane helix domains folded into an antiparallel dimer, where the orientation of the two domains is fixed by a single transmembrane linker helix. Using phylogenetic sequence conservation as a guide, we have identified several functionally important residues. There is substantial functional asymmetry in the effect of mutation at corresponding sites in the two domains. Specifically, mutations to residues in the C-terminal domain proved significantly more detrimental to function than did similar mutations in the N-terminal domain. Our data suggest particular residues that may be important to anion specificity, most notably the necessity of a positive charge near the end of TMH1 in the C-terminal domain. It is possible that a cationic charge at this location may create an electrostatic well for fluoride ions entering the channel from the cytoplasm.**

Fluoride is a toxic anion that is ubiquitous in both terrestrial and marine environments at concentrations that range from low micromolar to >100 mM (1–3). The harmful effects of high concentrations of fluoride have been documented for species from all domains of life (1, 4–8). Several essential proteins, including phosphoryl-transfer enzymes and enolases, are highly sensitive to fluoride (9–13), suggesting that most organisms must be equipped either to sequester or to export fluoride ions. It has recently been shown that archaeal, eubacterial, and eukaryotic genomes encode proteins that export fluoride from the cell, thereby protecting these organisms from its detrimental effects.

A major breakthrough in understanding fluoride biology came with the recent discovery of fluoride-responsive riboswitches in eubacteria and archaea. These noncoding RNAs regulate the expression of a diverse set of genes, including many that encode membrane proteins thought to be involved in ion transport (8). These have since been identified as fluoride exporters, and two distinct structural families are currently recognized. The first, called $CLC^F$, is a variant in the CLC superfamily, known for the transport or channeling of chloride ions. $CLC^F$ genes encode $F^-/H^+$ antiporters in eubacteria and are generally under the control of $F^-$-sensitive riboswitches (8, 14).

The second, much more broadly distributed family is called Fluc in bacteria (formerly *crcB*) (15) and FEX[2] in eukaryotes (16). Several Fluc proteins have been demonstrated to function as *bona fide* ion channels that can discriminate against the chloride ion with >10,000-fold selectivity (15). Among eukaryotic systems, *Saccharomyces*, *Candida*, and *Neurospora* have been shown to depend upon FEX proteins for resistance to fluoride (16), but neither the mode of transport nor the anion selectivity of those proteins has been established. *S. cerevisiae* contains two nearly identical FEX proteins (Fex1p and Fex2p) that maintain a low fluoride concentration in the cell, even under external fluoride assault. Without these proteins, yeast are 1000-fold more sensitive to the toxic effects of fluoride and would be

* This work was supported, in whole or in part, by National Institutes of Health Grants GM60696 (to C. S.) and GM022778 (to S. A. S.). The authors declare that they have no conflicts of interest with the contents of this article.
[S] This article contains supplemental Table S1.
[1] To whom correspondence may be addressed: Dept. of Molecular Biophysics and Biochemistry, Dept. of Chemistry, Yale University, P.O. Box 208114, New Haven, CT 06520. Tel.: 203-432-9772; Fax: 203-432-5767; E-mail: scott.strobel@yale.edu.

[2] The abbreviations used are: FEX, fluoride exporter; TMH, transmembrane helix; 4TMH, four-transmembrane helix; SMR, small multidrug resistance protein; Dom1, domain 1; Dom2, domain 2; gGFP, glycosylatable form of GFP; AUC, area under the curve; TM, transmembrane.

unable to survive in many environmental conditions, including most municipal tap water (16).

Prokaryotic Fluc proteins have an unusual dimeric structure that has not previously been observed among ion channels. Each monomer includes four transmembrane $\alpha$-helices, and the active molecule is an antiparallel dimer (15, 17) resembling the small multidrug resistance protein (SMR) EmrE (18, 19). These dimers can be formed either by a single protein species inserted into the membrane in both orientations or by two distinct protein monomers encoded by separate genes. A more constrained arrangement exists for eukaryotic FEX proteins, in which two nonidentical four-transmembrane helical (4TMH) domains are covalently joined by a single linker helix, effectively forcing an antiparallel orientation of the two principal domains (15, 16). Interestingly, artificially fused bacterial Fluc proteins engineered to display this 4 + 1 + 4 TMH topology also make functional fluoride channels (15). Given the differences in FEX structure between bacteria and eukaryotes, the following question arises. How conserved are the amino acid sequences among these proteins? Alignment of bacterial sequences shows several regions of conservation (15), and if the same amino acids are also conserved in eukaryotic FEX sequences, these residues are likely to be important for fluoride transport, either directly or indirectly.

Because the study of fluoride-export mechanisms is still at an early stage, many questions are yet to be answered, including several concerning the regulation of eukaryotic FEX genes. One possibility is regulation by riboswitch-like elements, as seen in bacteria. Alternatively, *FEX* might be modulated by toxin-sensing transcriptional regulators, as for the arsenate transporter protein in *Saccharomyces*, ScAcr3 (20). Post-transcriptional regulation is also possible, either at the level of translation, such as for the multidrug resistance transporter, ScHol1 (21, 22), or at the level of directed targeting, as for the cadmium exporter ScPca1 (23–25). An additional question exists as to whether limited resistance to fluoride might be gained by shunting this anion to the yeast vacuole, a mechanism of detoxification for several metals (20). Measuring FEX RNA and protein levels and visualizing the cellular membranes with which FEX protein associates should provide answers to these important questions.

Here, we establish that FEX proteins in *Saccharomyces cerevisiae* are constitutively expressed in the plasma membrane and are directly responsible for fluoride extrusion, without the need for vacuolar sequestration. We also define the transmembrane topology of the protein and identify conserved residues that are critical for function in the first and second transmembrane segments.

## Experimental Procedures

*Yeast Strains and Growth Measurements*—The *S. cerevisiae* strains used in this study are listed in supplemental Table S1. All strains were maintained routinely on YPD or SD-ura medium (26, 27) and were prepared for experiments by overnight growth in liquid culture. For spot assays, cells were diluted to $A_{600} = 0.2$ and further serially diluted in sterile $H_2O$. Approximately 3 $\mu$l of cell suspension was spotted onto YPD or YPD + NaF plates and grown at 30 °C for several days prior to imaging. For liquid growth assays, cultures were diluted to $A_{600} = 0.1$ in Costar 24-well flat bottom plates containing YPD and varying concentrations of NaF in a final volume of 1 ml. $A_{600}$ readings were taken at 3-min intervals until growth plateaued using a BioTek Synergy 4 plate reader set at 30 °C with continual shaking. To determine $IC_{50}$ values, the area under the curve (AUC) was calculated for each growth curve. AUC values were normalized relative to the appropriate growth curve with no fluoride. These relative AUC values were plotted *versus* the log of the fluoride concentration and fit to a standard dose-response curve with GraphPad Prism to extract $IC_{50}$ values. To calculate the relative $IC_{50}$ values plotted in Fig. 11, the $IC_{50}$ value for each mutant was divided by that for the wild type. All $IC_{50}$ values reported are the average of at least three trials, and the error reported is the standard deviation.

*Electrophysiology*—Yeast strains with enlarged cells have proven especially useful for patch clamp measurements (28, 29), particularly strains deleted of the calcium transporter (Pmr1p) that normally resides in Golgi membranes (30). Therefore, all strains used here to assess FEX currents were *pmr1*Δ as follows: the "wild type," *FEX1 FEX2 pmr1*Δ; the double knock-out, *fex1*Δ *fex2*Δ *pmr1*Δ; and both single knock-out strains. Cells were grown to mid-log phase ($A_{600} \approx 2$; overnight at 25 °C), harvested by centrifugation, washed twice in phosphate-$\beta$ME buffer (50 mM $KH_2PO_4$, pH 7.2, 0.2% $\beta$-mercaptoethanol), and processed as described previously (28). Briefly, 3 ml of washed cells were resuspended in phosphate-$\beta$ME buffer, preincubated for 30 min (30 °C, with rotation at 60 rpm), spun down again, resuspended in the same buffer + 1.2 M sorbitol + 0.6 units of Zymolyase 20T (catalog no. 320921, IMP Biomedicals, Inc., Irvine CA), and incubated for 45 min (also 30 °C at 60 rpm). The resultant spheroplasts were pelleted and resuspended in a slightly hypotonic stabilizing buffer (220 mM KCl, 10 mM $CaCl_2$, 5 mM $MgCl_2$, plus 5 mM MES titrated to pH 7.2 with Tris base, + 0.2% glucose). These suspensions were stored stationary (room temperature, ~23 °C) for up to 8 h and used for whole-cell patch recording. For the patch clamp measurements, ~5 $\mu$l of suspension was pipetted into the recording chamber, allowed to settle for ~10 min, and then flushed with a stream of standard recording buffer (Buffer D: 150 mM KCl, 10 mM $CaCl_2$, 5 mM $MgCl_2$, 1 mM MES, pH 7.5), to remove debris and nonadherent cells. Slightly alkaline buffers were used throughout the measurements for three explicit reasons as follows: (i) to suppress spurious movement of fluoride via HF, the undissociated acid ($pK_a = 3.2$); (ii) to suppress fluxes of inorganic cations via Kch1,2p and other nonselective "channels" through the yeast plasma membrane (31, 32); and (iii) to minimize confusing halide conductance facilitated by the TRK1 and TRK2 $K^+$ transporters (29). Visibly clean protoplasts of ~8 $\mu$m diameter were selected under bright field illumination (×400) and picked by the patch pipette, using suction at ~8 cm of $H_2O$.

Patch pipettes were fabricated from 1.2-mm borosilicate capillaries (Kimax051, Kimble/Kontes 38500) using a two-step Narishige puller (model PC-10), then fire-polished into a pointed dome, with a tip diameter of ~1.5 $\mu$m. The polished pipettes were filled with different "intracellular" buffers. All filling solutions were prefiltered through 0.2-$\mu$m acrodiscs (catalog no. 4454, Pall Corp., Ann Arbor, MI). Buffer G:8-$Cl^-$ con-

tained 8 mM KCl, 175 mM potassium gluconate, 1 mM EGTA, 4 mM $K_2ATP$, 10 mM magnesium gluconate, and 0.3 mM calcium gluconate, titrated to pH 7.0 with KOH. To prepare similar solutions containing varied concentrations of fluoride or chloride, potassium gluconate was replaced by a molar equivalent of potassium fluoride or KCl. However, simple potassium fluoride-filled pipettes quickly degraded with a floccular coating when dipped directly into Buffer D, due to the low solubility products of $CaF_2$ and $MgF_2$ ($\sim 10^{-9}$). This problem was avoided by filling the pipette in two steps. First, ~0.03 $\mu$l of Buffer G:8-Cl was sucked into the tip of each pipette; second, ~3 $\mu$l of fluoride-containing buffer was injected (back-filled) into the pipette's shank, while the tip was held in air. The pipette tip was quickly submerged and pushed to the protoplast surface in <30 s for picking and to initiate gigaseal formation. Gigaseals formed on usable cells (~60% of trials) within ~5 min and were allowed to stabilize for another 5–10 min. Whole-cell recording was obtained via a high voltage pulse (750 mV, 100 $\mu$s) coupled with brief doubling of suction pressure. Control of the voltage clamp protocol, collection of current data, and preliminary analysis were carried out via an EPC9 amplifier and Pulse software (HEKA Elektronik, Lambrecht, Germany), interfaced with a PowerMac G4 microcomputer. All voltage scans were generated from a holding voltage of −40 mV, clamping in 1.5-s pulses and 20-mV decrements from +20 mV to −180 mV, as illustrated in the superimposed voltage traces of Fig. 1*A*. Data were collected at 2 kHz and filtered at 250 Hz.

*FEX Protein Quantification*—To facilitate protein detection by immunoblotting, an HA tag was cloned onto the C terminus of *FEX1* and *FEX2* by homologous recombination of three overlapping PCR fragments as described below for the GFP fusions. The sequence of the tag was amplified from the plasmid pAG426GPD-ccdB-HA (a gift from Susan Lindquist; Addgene plasmid number 14252). A five-amino acid linker (SLGGM) was added between the C terminus of Fex1,2p and the HA tag. These resulting plasmids, pRS416-*FEX1-HA* and pRS416-*FEX2-HA*, were transformed into SSY3, and their function was tested *in vivo*. The sequence of HA-tagged *FEX1* or *FEX2* was also inserted into the yeast genome as described below for GFP-tagged *FEX*1. The resulting strains, SSY21 and SSY22 (supplemental Table S1), were mated and sporulated, and the resulting tetrads were dissected to isolate a strain in which both *FEX1-HA* and *FEX2-HA* were integrated into their native loci (SSY23). These strains were then used to quantify the amount of FEX protein as follows.

Plasma membranes were prepared as described previously (33), starting with 450 OD of cells grown overnight to mid log phase. Cells were harvested by centrifugation (5 min at 5000 rpm in a GSA rotor), resuspended in 30 ml of lysis buffer (50 mM Tris-HCl, pH 7.5, 0.3 M sucrose, 5 mM $Na_2EDTA$, protease inhibitor cocktail: PIC = 1 mM phenylmethylsulfonyl fluoride plus 2.5 mg/ml chymostatin), and passed through a French press at 20,000 p.s.i. The resultant slurry was spun for 5 min at 4000 rpm in the Sorvall SS34 rotor, decanted into clean tubes, and spun again for 10 min at 11,000 rpm (14,000 × *g*). Supernatants were then decanted and spun for 35 min in the Ti50.2 ultracentrifuge rotor, at 43,000 rpm (200,000 × *g*). The final supernatant was aspirated, and the pellet (crude plasma membranes) was added to 2 ml of membrane wash buffer (10 mM Tris base, 1 mM $Na_2EDTA$, 1 mM EGTA, 20% (w/v) glycerol, 1 mM DTT, plus PIC, adjusted to pH 7.0) and then resuspended via a motorized Teflon-glass homogenizer. The mixture was then loaded onto an iced sucrose step gradient (54:65%, w/v) and spun in the SW55Ti rotor at 44,000 rpm for 2 h (~220,000 × *g*). After removal of the upper layers by aspiration, the cloudy lower band and interface material (about 2 ml) was collected and diluted into 20 ml of 1 mM EGTA/Tris, pH 7.5, plus PIC, in a Ti50.2 tube. After a final spin at 43,000 rpm for 35 min, the supernatant was aspirated off, and the translucent plasma membrane pellet was resuspended in 100 $\mu$l EGTA/Tris, pH 7.5, plus PIC, and then stored at −70 °C.

Western blotting was conducted as demonstrated in Fig. 2, calibrating sample band intensities by means of HA-tagged plasma membrane ATPase (ScPma1-HA; enzyme provided by A. B. Mason) as described previously (34). Samples were assayed for total protein content using the Lowry method (35), before being electrophoresed on precast polyacrylamide gradient gels (4–15% TGX gel 456–1086; Bio-Rad), and then stained for 1 h with primary anti-HA monoclonal antibody (MMS-101P, Covance Corp., Berkeley, CA) and for a 2nd h with anti-mouse antibody coupled to horseradish peroxidase (HRP; 4021, Promega Corp., Madison, WI). Blots were visualized with Denville HyGlo ECL reagent (E2400; Denville Scientific, Metuchen, NJ) and Kodak XAR autoradiographic film, imaged on a CanoScan 8400 at 600 dpi, and analyzed via ImageQuant software (GE Healthcare).

*Cloning and Imaging of GFP-tagged FEX*—To identify a functional GFP-tagged Fex1p for localization studies, GFP was inserted at several positions as follows: the N and C termini and in the loop connecting TMH4 and TMH5 (L4/5) between amino acids 165 and 166 (165-GFP). To avoid potential problems with localization, the first 15 amino acids of Fex1p were repeated upstream of GFP in the N-terminal construct. The C-terminal tag was added using PCR-mediated gene modification where the GFP sequence was amplified from pFA6a-GFP(S65T)-kanMX6 (36) and included homology to the 3′ end of *FEX1*. This PCR product was transformed into *fex2*Δ yeast (SSY10) using the standard lithium acetate procedure (37), and clones with GFP were selected by plating on G418. Correct tagging was confirmed by PCR amplification and sequencing of *FEX1*. The other GFP constructs were made using three overlapping PCR fragments that were assembled in *fex1*Δ *fex2*Δ yeast (strain SSY3 from (16)). Fragments containing the *FEX* sequence were amplified from pRS416-*FEX1* (16), and those containing GFP were amplified from pFA6a-GFP(S65T)-kanMX6. The end fragments contained 50 bases of homology to the pRS416/pRS426 vector backbone (centromeric/2 $\mu$), which was digested with HINDIII and transformed into SSY3 along with the three fragments (38, 39). Yeast that successfully assembled the fragments and vector were isolated on SD-ura media, and their DNA was isolated, transformed into *Escherichia coli,* and verified by sequencing of each resulting plasmid. Yeast harboring plasmids with the correct sequence were tested for GFP fusion protein functionality using the liquid growth assay described above. Both the N-terminal and 165-GFP proteins were active with $IC_{50}$ values near wild type

(Table 1). In contrast, the C-terminal construct showed significantly decreased activity and was therefore not used further.

To construct a yeast strain with GFP-tagged *FEX1* integrated into the genome, the coding region of each construct was amplified from the plasmid along with 45 nucleotides of the upstream and downstream regions and transformed into SSY3. These yeast were plated on YPD, grown overnight at 30 °C, and replica plated on YPD + 500 μM NaF. Colonies were isolated after 2–3 days of growth and streaked on YPD + G418 and YPD + hygromycin B (both at 300 μg/ml). In SSY3, the *FEX1* locus is replaced with the kanMX6 cassette and the *FEX2* locus with the hphMX4 cassette. Therefore, successful re-integration of GFP-tagged *FEX1* at the correct locus would cause a loss of G418 resistance while retaining hygromycin resistance. Strains satisfying these criteria were isolated and confirmed via liquid growth in NaF-containing media.

To construct strains in which both *FEX1* and *FEX2* are tagged with a fluorescent protein, first *FEX1–165-GFP fex2*Δ *MATa, FEX1–165-mCherry fex2*Δ *MATa, fex1*Δ *FEX2–165-GFP MATα,* and *fex1*Δ *FEX2–165-mCherry MATα* strains were made using homologous recombination in SSY3 (FEX1 tags) or SSY4 (FEX2 tags) as described above. The sequence of mCherry was amplified from pFA6a-mCherry:natMX4 (a gift from Mark Hochstrasser). These strains were mated, sporulated, and dissected. Spores with the genotypes *FEX1–165-GFP FEX2–165-mCherry* and *FEX1–165-mCherry FEX2–165-GFP* were isolated by monitoring for loss of both G418 and hygromycin resistance.

For topology assignment, plasmids bearing *FEX1* were constructed with gGFP inserted into several intracellular and extracellular loops, as well as onto the N terminus, using the high copy vector, pRS426. The high copy vector was used to amplify the fluorescent signal. Each construct was assembled by homologous recombination in SSY3 as described above using three overlapping PCR products and linearized pRS426. The sequence of gGFP was amplified from p424GPD yEGFP E172T HA, a gift from Gunnar von Heijne and Hyun Kim (40). The following sites in the FEX1 protein were successfully tagged, after each amino acid: Gly-113 (L3/4), Phe-165 (L4/5), Arg-238 (L5/6), Thr-299 (L7/8), and at the N terminus. Similarly to the wild-type GFP constructs, the first 15 amino acids of Fex1p were repeated upstream of GFP in the N-terminal gGFP plasmid. The functionality of all tagged proteins was assessed using the liquid growth assay (Table 2).

*Fluorescence Imaging*—Yeast bearing GFP, gGFP, or mCherry were grown to mid-log phase (4–5 h, shaking at 30 °C) in YPD, washed twice in SD media, and spread very thinly on 1.2% agarose pads (containing SD medium). Slides were mounted on the stage of a Nikon Ti-E inverted microscope and visualized with a CFI Plan-Apo Lambda ×100 DM, NA 1.45, objective, under oil immersion at room temperature (~23 °C). Images were recorded on an Andor Clara Interline digital camera and contrast-enhanced with Nikon Elements software.

*FEX Regulation, Northern Blots*—Total RNA was obtained using the Ambion RiboPure kit according to the manufacturer's directions. 10 μg/sample of total RNA was run on 1.2% denaturing agarose gel, and RNA was transferred to a positive-charged nylon membrane (Amersham Biosciences, Hybond-$N^+$) using standard techniques. The sequence of *FEX1* was amplified using PCR, and this product was labeled with [$\alpha$-$^{32}$P]dCTP (PerkinElmer Life Sciences) using random hexamer primers and the Klenow fragment enzyme (New England Biolabs). This labeled probe was hybridized to the membrane with Hyb-LINK (G Biosciences) using standard techniques. The blots were exposed to phosphor screens and read with a Storm Molecular Imager using ImageQuant software.

*Western Blots*—The *FEX1-HA fex2*Δ yeast strain was grown in 200 ml of YPD to log phase (~OD = 1.5), and cells were then incubated with 20 mM NaF for 10, 60, 90, and 120 min at 30 °C before harvesting by centrifugation (total time in the shaker was 9 h for all samples). Plasma membranes were prepared using a modification of the procedure described above. Briefly, cells were harvested by centrifugation at 1900 × *g* for 5 min and resuspended in Buffer A (50 mM Tris, pH 7.8, 0.3 M sucrose, 5 mM EDTA, 1 mM EGTA) supplied with freshly prepared protease inhibitor mixture (aprotinin 10 μg/ml, leupeptin 10 μg/ml, pepstatin 10 μg/ml, chymostatin 25 μg/ml, and phenylmethylsulfonyl fluoride 250 μg/ml). The cells were lysed with glass beads using a Beadbeater (Biospec) with 3 pulses of 30 s each. Cell lysate was spun at 1900 × *g* for 5 min, and the supernatant was then spun at 14,000 × *g* for 10 min. This supernatant was decanted to a clean tube and spun at 45,000 × *g* for 40 min in a 70 Ti rotor (Beckman Ultracentrifuge) to pellet crude membranes. These membranes were resuspended in 50 μl of Buffer A with protease inhibitors, and total protein content was measured using the BCA kit from Pierce. 20 μg of total protein/sample were run on a 4–15% TGX gel from Bio-Rad. FEX1-HA protein was detected with a 1:1666 dilution of the primary HA.11 clone 16B12 monoclonal antibody from Covance (MMS-101P), and PMA1 was detected as a control using a 1:1000 dilution of the 40B7 antibody from Kamiya (MC-025) followed by incubation with secondary anti-mouse IgG conjugated with HRP (Promega) in a 1:5000 dilution.

*Cloning of FEX1 Dom1 and Dom2 and E. coli Fluc*—To make the Dom1 construct, the sequence of amino acids 1–148 and 362–375 of *FEX1* was amplified from pRS416-*FEX1* and inserted into the overexpression vector p426GPD (41) using Gibson Assembly (New England Biolabs). Similarly, to construct Dom2, the sequence of amino acids 1–10 and 241–375 of *FEX1* was amplified and inserted into p426GPD. In both cases, care was taken to ensure that there was no significant K + R bias that would drive membrane insertion in one orientation over the other. To make the Fluc construct, the sequence of Fluc from *E. coli* strain BW25113 (ORF BW25113_0624) was amplified from genomic DNA with primers that included the first 10 amino acids of *FEX1* to potentially help with correct localization. This sequence was inserted into p426GPD using Gibson Assembly (New England Biolabs). All three constructs were transformed into SSY3 and tested for growth by streaking on YPD plates containing 5 mM NaF as well as by the liquid growth assay described above.

*Cloning of FEX1 Mutants*—Site-directed mutagenesis was performed on the pRS416-*FEX1* plasmid (16) using the QuikChange II site-directed mutagenesis kit (Agilent) according to the manufacturer's directions. Briefly, DNA oligonucleotides were designed with the specific mutation flanked by ~20

bp with perfect homology to upstream and downstream of the point mutation. The presence of the mutation was verified by sequencing. SSY3 was transformed with pRS416, pRS416-*FEX1*, or pRS416-*FEX1* mutant plasmids, and transformants were isolated on SD-ura media.

## Results

*FEX1 and FEX2 Produce Fluoride Conductance in the Plasma Membrane*—With FEX1 and/or FEX2 proteins expressed at constitutive levels, whole-cell patch clamping of *S. cerevisiae* membranes demonstrated huge fluoride-ion currents consistent with both proteins functioning as fluoride channels. Currents with either/both were much larger than the steady-state currents of the plasma membrane proton pump (Pma1p), which energizes most ion transport at the yeast surface. As shown in Fig. 1, when $[F^-]_I$ = 75 mM, the expected resting membrane voltage of −180 mV drove an average inward current of ~65 pA through each protein. Thus, when expressed separately, the two FEX proteins functioned at the same level. With simultaneous expression of both proteins, we measured a current of ~110 pA at −180 mV, less than a simple addition of the currents produced by the two proteins expressed individually (Fig. 1). Residual current with the FEX proteins deleted (Fig. 1) was ~5%.

To calculate the rate of ion turnover, an estimate of the number of FEX molecules per cell is needed. We determined the amount of FEX protein in yeast plasma membranes using quantitative Western blotting with HA-tagged versions of Fex1p and Fex2p and a calibration standard (34). When expressed separately, Fex1p and Fex2p are present in yeast membranes at the same level, 1.7 or 1.8 fmol/$\mu$g of membrane protein, respectively. When both proteins are present, we measured 2.4 fmol/$\mu$g of membrane protein (Fig. 2). In agreement with our electrical measurements, simultaneous expression of both genes reduces the amount of each by a modest fraction, implying a weak regulatory interaction between the two FEX genes or proteins.

The plasma membrane preparations yielded ~1330 $\mu$g of membrane protein for $6.3 \times 10^9$ cells, meaning ~220 molecules of Fex1p or Fex2p per cell in the single expressing strains or ~310 molecules per cell in the wild type. Given the corresponding measured currents of 65 or 110 pA, per-site currents or turnover numbers are $1.9 \times 10^6$ ion/s for the single expressing strains and $2.3 \times 10^6$ ions/s for the wild type. These numbers compare with ~$10^7$ $F^-$ ions/s via the bacterial channel FlucEc2 (15), and they are in range for conventional ion channels. FEX currents driven by the voltage clamp at lower fluoride concentrations fell approximately linearly with concentration, so at quasi-physiological concentrations (~1 mM or lower), average per-site turnover numbers would fall in or below the neighborhood of $10^4$ ions/s (Fig. 3).

FEX proteins are selective for fluoride over chloride, albeit to a lesser degree than Fluc proteins. The measured current when the intracellular (pipette) solution contains only chloride (but FEX proteins still present) is ~15% of that when fluoride is in the pipette, as summarized by the averaged current-voltage (*I-V*) plots in Fig. 1*B*. These numbers imply a selectivity ratio somewhat greater than 10:1 for $F^-/Cl^-$, weaker than has been reported for the Fluc protein purified from *E. coli* (~10,000:1 (15)). However, it is likely that a large fraction of the discrepancy owes to spurious conductance pathways, such as residual $Cl^-$ flux through the TRK proteins at alkaline pH (29).

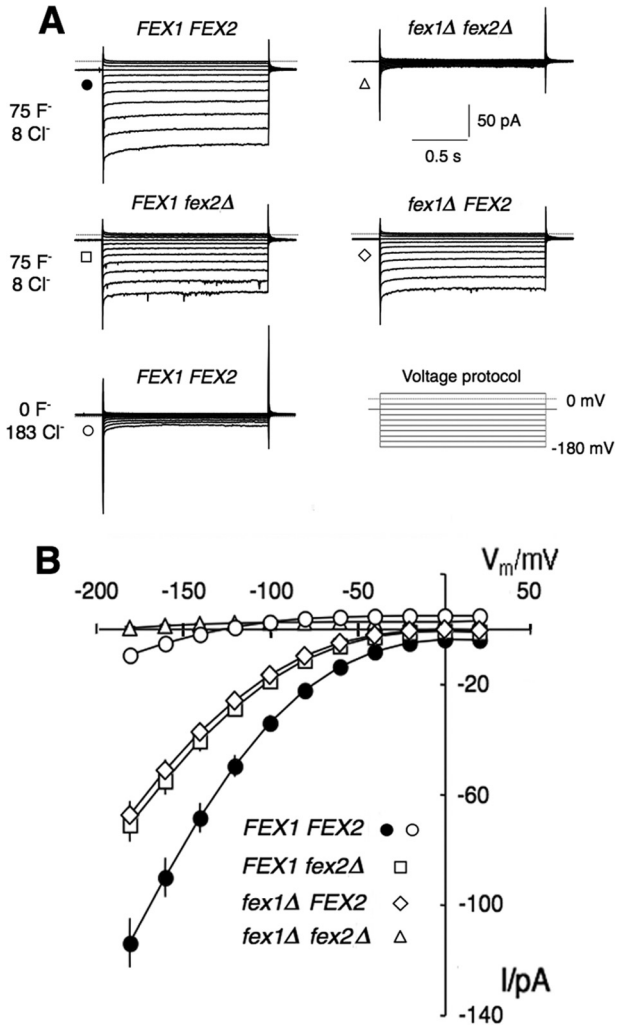


FIGURE 1. **Both yeast FEX proteins conduct channel-like currents in the presence of cytoplasmic fluoride.** *A*, currents measured via whole-cell patch clamping on representative yeast spheroplasts from four different strains as follows: WT for both FEX genes (*left column, top panel*); knock-out of both FEX genes (*right column, top panel*); knock-out of *FEX2* (*left column, middle panel*); and knock-out of *FEX1* (*right column, middle panel*). The standard condition used 75 mM potassium fluoride in the pipette (cytoplasmic) solution and that yielded maximal steady-state currents between −48 and −86 mV for both single knock-out strains and between −78 and −143 pA in WT cells examined (at −180 mV). Residual current under the same conditions but absent in both FEX genes/proteins was ~5%; residual current with full salt replacement by KCl was ~15%. Recorded traces were not corrected for leakage currents. Currents for typical scans are shown as stacked 1.5-s traces, with negative (downward) currents designating cation flux from the bath to the cell interior. Heavy traces continued to the left and right of each stack represent clamp current at the holding voltage of −40 mV; *dotted lines* designate the current for zero voltage. *B*, plot of averaged currents for 6–8 separate cells for each strain, similar to those in *A*, *versus* clamped membrane voltage. Averages were calculated over the last 500 ms of each trace, pre-corrected for leakage currents (29). *Error bars* designate 1 S.E. $pH_i$ = 7.0 in all cases, and salt for osmotic balance was potassium gluconate. External solution, Buffer D, pH 7.5 (see experimental procedures). All four yeast strains carried a deletion of the *PMR1* gene (*pmr1*Δ) a Golgi-resident calcium pump (30), which produces enlarged cells for easy patch clamping. Very small apparent positive currents at low voltages are a leakage artifact.

Two additional properties of the FEX currents are noteworthy. First, the ion currents relaxed about 30% over the first

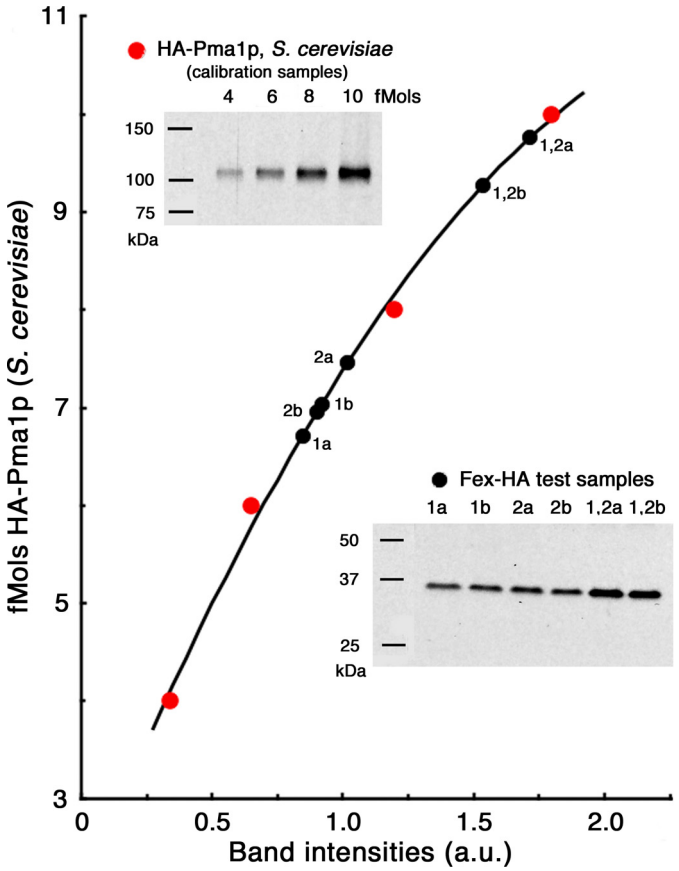


FIGURE 2. **Quantification of FEX proteins in yeast plasma membranes.** *Lower inset,* Western blot of HA-tagged Fex1p and Fex2p. Each band represents 4 $\mu$g of membrane protein. *1a* and *1b* are samples from *FEX1-HA; 2a* and *2b* are samples from Δ*fex1 FEX2-HA; and 1,2a* and *1,2b* are samples from *FEX1-HA FEX2-HA. Upper inset,* Western blot of HA-tagged *Saccharomyces* Pma1p (calibrating standard) in known ratio (20%) to the partially purified membrane protein. 2–5 ng of the standards contained 4, 6, 8, and 10 fmol of Pma1p-HA, respectively, for the four plotted *red points*. The (least squares) parabola $= -1.18X^2 + 6.54X + 2.02$, fitted to the *red* points, was used for direct calculation of femtomoles of HA associated with each protein sample of Fex1p or Fex2p. *a.u.,* arbitrary units.

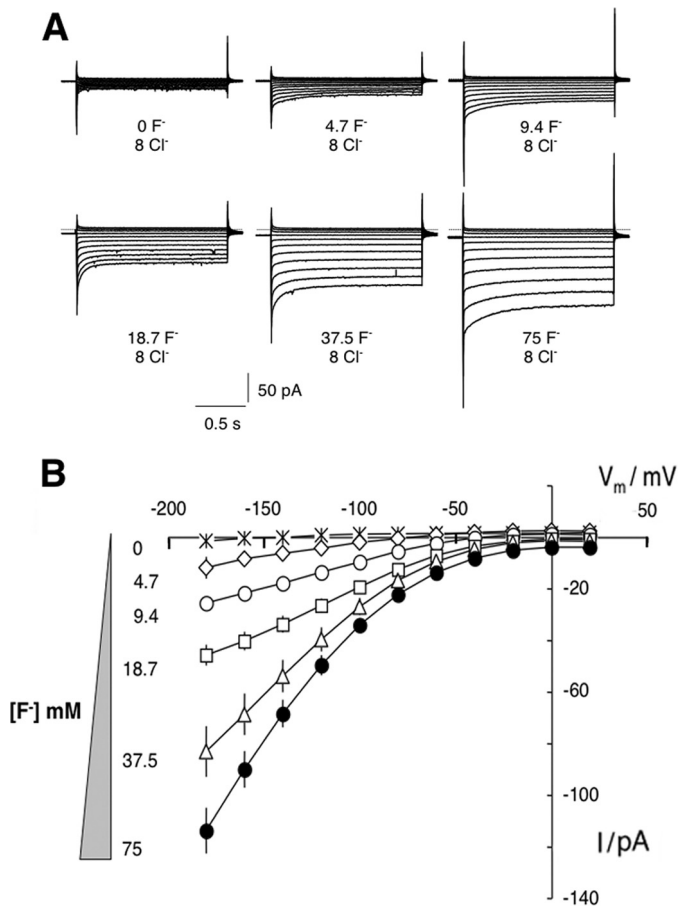


FIGURE 3. **FEX-mediated currents vary with cytoplasmic fluoride concentration.** *A,* representative traces of whole-cell currents from different spheroplasts, for experiments similar to that in Fig. 1*A* but with differing $[F^-]_i$ in the patch pipette. *B,* current-voltage relationships averaged for the full set of experiments. Plot of pA *versus* $[F^-]_i$ at −180 mV fits a Michaelis curve with $K_{0.5}$ ~64 mM. Yeast strain is as follows: *FEX1 FEX2 pmr1*Δ. $[Cl^-]_i$ was kept at 8 mM throughout, and osmotic balance was maintained by potassium gluconate. *Error bars* are S.E. values for $n = 7, 5, 6, 8, 3$, and 1 trials on different cells, with $[F^-]_i = 75, 37.5, \ldots, 4.7$, and 0 mM, respectively.

~400 ms of each clamp step, indicating an unusual kinetic complexity. Second, the slope conductances ($dI/dV$) of the steady-state currents became approximately constant as membrane voltage was clamped increasingly negative to −120 mV (Figs. 1*B* and 3*B*). The latter finding suggests the presence of a conventional channel-gating process, even though no on-off switching was visible in the actual current traces (Figs. 1*A* and 3*A*).

*FEX Protein Is Located in the Plasma Membrane*—Localization of the FEX proteins in the yeast plasma membrane is logically required by the patch clamp measurement of FEX-dependent currents through that membrane. This localization is reinforced by the results in Fig. 2, demonstrating abundant FEX protein in the yeast plasma membrane fraction. FEX protein co-purifies substantially with the well-established plasma membrane protein Pma1p, under conditions essentially free of proteins originating from the cytosol, mitochondria, or other organelles (*e.g.* NADPH cytochrome *c* reductase activity in the purified plasma membranes <0.5% of the total cell lysate; data not shown). Furthermore, FEX can also be directly visualized at the plasma membrane using fluorescent tags. We have made several fusions of Fex1p with green fluorescent protein (GFP) and imaged cells expressing these fusions using fluorescence microscopy. GFP was inserted at the N and C termini and in the central loop between TM4 and TM5, L4/5 (165-GFP). All constructs were tested for function using solid and liquid growth assays. Both the N-terminal and 165-GFP fusion proteins behave similarly to wild-type Fex1p, but the C-terminal fusion was not functional (Fig. 4*A* and Table 1). Identical results were obtained when *FEX2* was tagged in L4/5 (Table 1).

GFP fluorescence locates the FEX proteins at the plasma membrane of *S. cerevisiae*, where punctate spots ring the exterior edge of the cells (Fig. 4*B*). This clustering and localization are independent of the particular GFP construct (FEX1 or FEX2, N-terminal GFP or 165-GFP, expressed from the chromosome or from a centromeric plasmid; Fig. 4*B* and data not shown) and were exaggerated into a dense paracellular ring by expression from a high copy plasmid (Fig. 4*B*). Although our data cannot completely rule out the possibility that some fraction of the protein is associated with cortical endoplasmic reticulum, the function of Fex1p, its purification in the plasma membrane fraction, and the electrical measurements presented

**TABLE 1**
**$IC_{50}$ values for GFP and HA-tagged strains**

| Strain | $IC_{50}$ |
|---|---|
| | mM |
| pRS416-*FEX1* | 56 ± 7[a] |
| pRS416-*N-GFP-FEX1* | 68 ± 3 |
| *FEX1-C-GFP fex2Δ* | 0.43 ± 0.02 |
| pRS416-*FEX1–165-GFP* | 49 ± 2 |
| pRS426-*FEX1–165-GFP* | 57 ± 4 |
| *FEX1–165-GFP fex2Δ* | 37 ± 3 |
| *fex1Δ FEX2–165-GFP* | 37 ± 2 |
| *FEX1-HA fex2Δ* | 56 ± 8 |
| *FEX1-GFP FEX2-mCherry* | 52 ± 2 |
| *FEX1-mCherry FEX2-GFP* | 50 ± 3 |

[a] All values are the average of at least three trials ± S.D.

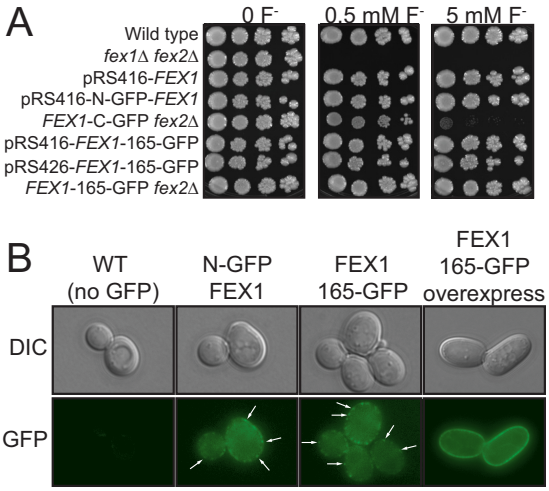


FIGURE 4. **Fex1p is localized at the yeast plasma membrane.** *A,* growth of GFP-tagged FEX1 strains on several concentrations of NaF. *B,* images of yeast strains with and without GFP-tagged FEX1. *White arrows* show examples of punctate GFP expression. Images of WT, N-GFP-FEX1, and FEX1–165-GFP were taken with a 3-s exposure for fluorescence and a 150-ms exposure for differential interference contrast (*DIC*). Overexpression was imaged by a 500-ms exposure for fluorescence.

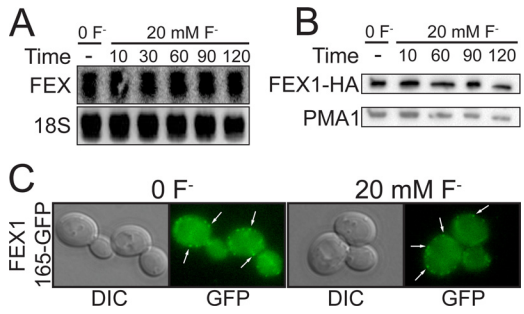


FIGURE 5. **FEX is constitutively expressed in actively growing yeast.** *A,* Northern blot showing mRNA levels of FEX1 and FEX2 as a function of time of exposure to NaF. *B,* Western blot showing the corresponding protein levels of FEX1. *C,* demonstration that localization of Fex1p does not change in the presence/absence of fluoride. Images taken using a 5-s exposure for fluorescence and 150-ms exposure for differential interference contrast (*DIC*).

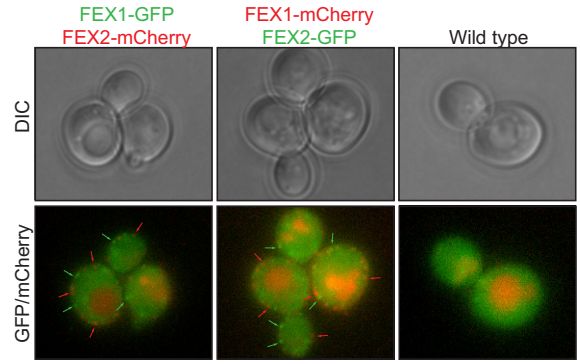


FIGURE 6. ***FEX1* and *FEX2* are expressed at visually equivalent levels.** Fluorescent imaging of strains with both Fex1p and Fex2p labeled is shown. *Arrows* show representative examples of GFP and mCherry fluorescence. *DIC,* differential interference contrast.

above strongly support localization in the yeast plasma membrane.

*FEX Proteins Are Constitutively Expressed*—To conserve biosynthetic effort, many proteins (particularly transport proteins dealing in scarce or rare agents) are tightly regulated, often being synthesized or activated only when needed. Given this general fact and, furthermore, that many bacterial Fluc proteins are up-regulated when fluoride is present, we sought to determine whether the expression of FEX is regulated by fluoride. Many of the prokaryotic fluoride channels are regulated by riboswitches, noncoding RNAs that control gene expression at the transcriptional or translational level in response to the binding of a small molecule or ion (8, 42). Very few eukaryotic riboswitches have been demonstrated, and in the specific case of *FEX1,2,* no obvious candidate sequence has been found. However, because many other transport-regulatory pathways exist in yeast that could regulate the production of *FEX* in the presence of fluoride ions, we looked more broadly at mRNA and protein production and localization as a function of fluoride exposure.

FEX proteins are constitutively expressed in actively growing yeast, but neither FEX protein nor FEX mRNA is up-regulated in response to fluoride ions (Fig. 5). We extracted total RNA as well as plasma membrane proteins from actively growing yeast after various times of exposure to a large quantity of fluoride (20 mM). In all cases, the samples were identical to those extracted from yeast in culture with no added fluoride. Furthermore, we observed no change in the amount of fluorescence or localization of FEX1-GFP upon addition of fluoride to yeast cultures (Fig. 5*C*). Although for simplicity the majority of our studies have probed *FEX1*, fluorescence data from strains where both Fex1p and Fex2p are labeled with different fluorescent proteins indicate that both proteins are expressed at visually similar levels (Fig. 6), consistent with the protein quantification data presented above.

*Membrane Topology of FEX*—Based on the structure of bacterial Fluc proteins, it is expected that yeast Fex1,2p will be folded into an antiparallel dimer of homologous 4TMH domains, an arrangement forced by the extra transmembrane helix (TM5) that joins the two domains. Visual inspection of the Fex1p sequence using the K + R rule (43), and prediction by the TMHMM (44) and Phobius (45) programs all led to the same overall topology for Fex1,2p, with similar TMHs. The resultant model (Fig. 7*A*) locates the N terminus in the cytoplasm and the C terminus in the extracellular space and places the large linker, L4/5, in the cytoplasm, suggesting that a major role for that long (and conspicuously charged) central loop is to enforce the overall orientation of the FEX protein in the membrane.

To test this topological model, we utilized gGFP (40). This protein has an engineered glycosylation site located near the

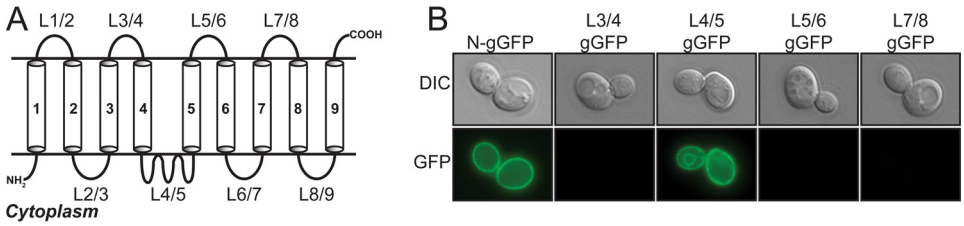


FIGURE 7. **Fex1p is folded as an antiparallel dimer.** *A,* topology model as predicted by the PHOBIUS (43) and TMHMM (42) programs. *B,* images of five strains expressing gGFP-tagged FEX1. The absence of fluorescence implies that the GFP tag is extracellular; the presence of fluorescence implies that the tag is intracellular. All images were taken with a 500-ms exposure for fluorescence and a 150-ms exposure for differential interference contrast (*DIC*).

**TABLE 2**
**$IC_{50}$ values and localization results for FEX1-gGFP fusions**

| Location of gGFP | $IC_{50}$ | Predicted location (in/out) | Experimentally determined location (in/out) |
|---|---|---|---|
| | *mM* | | |
| N-terminus | 69 ± 2[a] | In | In |
| L3/4 (Gly-113) | 60 ± 2 | Out | Out |
| L4/5 (Phe-165) | 59 ± 3 | In | In |
| L5/6 (Arg-238) | 70 ± 3 | Out | Out |
| L7/8 (Thr-299) | 35 ± 3 | Out | Out |

[a] All values are the average of at least three trials ± the standard deviation.

fluorophore, such that when the site is modified with a sugar, GFP fluorescence is suppressed. Because protein glycosylation takes place in the endoplasmic reticulum lumen but not the cytoplasm, gGFP located in the cytosol remains fluorescent, whereas gGFP located elsewhere (endoplasmic reticulum lumen or extracellular space) becomes glycosylated and nonfluorescent (40). This system provides a simple way to track the folding of transmembrane proteins.

For that purpose, we inserted gGFP at the N terminus and into several loops of Fex1p and imaged the fluorescence of cells bearing each separate construct. To increase the fluorescence signal, all gGFP-FEX1 fusions were expressed from a high copy plasmid. We also determined that all of the fusion constructs made functionally active protein (Table 2), indicating their correct cellular localization. The N-terminal and L4/5 FEX1-gGFP fusion proteins were highly fluorescent, confirming location of these sites in the cytoplasm (Fig. 7*B*). The remaining three constructs (L3/4-, L5/6-, and L7/8-gGFP) did not fluoresce, placing those three loops in the extracellular space (Fig. 7*B*). These results provide experimental verification for the FEX topology depicted in Fig. 7*A*.

*Domain Architecture*—Based upon the topology of Fex1p, the two homologous 4TMH domains (Dom1 and Dom2) are in an antiparallel orientation where the N and C termini of Dom1 are located in the cytoplasm, and the N and C termini of Dom2 are in the extracellular space (Fig. 8*A*). In many bacterial homologs, the functional dimer is formed by identical 4TMH polypeptides that can insert into the membrane in both orientations. So the following questions naturally arise. Could either Dom1 alone or Dom2 alone function as a spontaneous homodimer if expressed by itself? Or, has there been sufficient evolutionary drift so that each domain is now specialized for one specific orientation? Finally, could a bacterial 4TMH protein function in yeast?

To address these questions, we expressed Dom1 alone, Dom2 alone, and Fluc from *E. coli* and tested their ability to confer fluoride resistance to yeast with no endogenous FEX protein. All constructs contained the first 10 amino acids of Fex1p on the N terminus and approximately equal numbers of K + R residues on either side of the membrane to minimize orientation bias during insertion (Fig. 8*A*). All constructs were overexpressed using the glyceraldehyde-3-dehydrogenase (GPD) promoter.

Fluc from *E. coli* allowed growth on fluoride-containing media, but Dom1 or Dom2 alone did not (Fig. 8*B* and Table 3). Yeast expressing *E. coli* Fluc grew robustly on media containing 5 mM NaF, whereas those expressing either single FEX1 domain did not grow (Fig. 8*B*). Given that *fex1*Δ *fex2*Δ yeast cannot grow on media containing even 500 μM NaF (Fig. 4*A*), this demonstrates a significant ability of *E. coli* Fluc to function in yeast. To further quantitate this effect, we measured $IC_{50}$ values for fluoride for Fluc, Dom1, and Dom2, and we found that yeast expressing Fluc have an ~150-fold higher $IC_{50}$ than yeast with no fluoride exporter, whereas Dom1 and Dom2 provide no protective effect when expressed alone (Table 3).

*Conserved Motifs in FEX and Its Homologs*—The two-domain structure of eukaryotic FEX proteins makes an elegant mutagenic platform for structure-function analysis, because of the evolved sequence differences between the two "half"-molecules. This natural construct allows us to interrogate the contributions made by each monomer individually by examining the functional changes produced by mutation of single residues. That task is expected to be considerably more difficult in many bacterial homologs, where each single mutation changes two residues in the assembled functional protein.

To determine which residues may be most important for fluoride export, we identified protein regions that are conserved in homologs of *FEX* across all domains of life. We first performed an alignment of sequences from eukaryotes (~200 sequences) using the PROMALS3D alignment tool (46), which calculates a consensus sequence (Fig. 9*A*). A previously published alignment of bacterial sequences showed highly conserved regions in TM1, TM2, and TM3 and a more modest conservation in TM4 (15). When we compared our eukaryotic alignment to this, we observed similar trends, namely conservation of residues in TM1, TM2, and TM3 but no significant conservation in TM4. We chose to focus on residues that were conserved across distantly related sequences from eukaryotes, eubacteria, and archaea (Fig. 9).

In almost all sequences that we examined, the G*hhh*R motif in TM1 is conserved, although the Gly is an Ala in ~10% of Dom2 sequences, as is the case for yeast Fex1,2p. An Asn and Gly appear to be nearly universally conserved in TM2. A substantial segment (>10 residues) of TM3 is also conserved

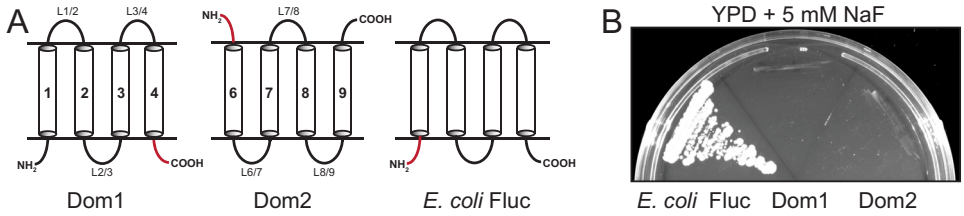


FIGURE 8. **Dom1 and Dom2 are not functional individually, but Fluc is active in yeast.** *A*, Dom1, Dom2, and Fluc from *E. coli*. The N- and C-terminal elements highlighted in *red* were cloned from *FEX1* to provide native termini. *B*, *fex1*Δ *fex2*Δ yeast expressing each construct from *A* were grown on YPD media containing 5 mM NaF.

**TABLE 3**
**$IC_{50}$ values for Dom1, Dom2, and *E. coli* Fluc**

| Strain | $IC_{50}$ |
|---|---|
| | *mM* |
| p426GPD (empty vector) | 0.033 ± 0.002[a] |
| p426GPD-Dom1 | 0.030 ± 0.002 |
| p426GPD-Dom2 | 0.027 ± 0.004 |
| p426GPD-Fluc | 9.9 ± 0.2 |

[a] All values are the average of at least three trials ± S.D.

across bacterial and eukaryotic Fluc/FEX proteins. There are a Gly and Ser that are nearly absolutely conserved, and although the other specific residues in this segment are somewhat variable across distantly related species, the region is clearly enriched for aromatic and hydroxylated residues (Fig. 9*A*).

To determine experimentally whether these conserved amino acids are essential for protein function, we mutated them singly in Dom1 alone, in Dom2 alone, and in both domains simultaneously. We measured the ability of yeast harboring each mutant FEX protein to grow in the presence of varying concentrations of fluoride. From these growth curves, $IC_{50}$ values were calculated for each mutant (Fig. 10; Table 4).

Mutations to residues in Dom2 affect FEX protein function to a much greater extent than mutations to Dom1, demonstrating that amino acids in Dom1 and Dom2 contribute asymmetrically to fluoride export. In each domain, we disrupted the G*hhh*R motif in TM1 by mutating Gly-29 to Ala (Dom1), Ala-251 to Gly (Dom2), and Arg-33 (Dom1) or Arg-255 (Dom2) to Ala. Additionally, we increased the spacing between the Gly and Arg by inserting a single Ala (32insA and 254insA). We also made alanine mutations of Asn-56 (Dom1) or Asn-277 (Dom2) in TM2 and Ser-97 (Dom1) or Ser-328 (Dom2) in TM3. From the $IC_{50}$ values for fluoride of these mutant proteins, we observe that mutations to Dom2 have a much greater effect on protein activity than do the corresponding mutations to Dom1 (Fig. 10 and Table 4). Indeed, the only mutation to Dom1 that has a significant effect is the addition of a single Ala to the G*hhh*R motif (▼ in Fig. 10*A*). In contrast, the R255A (◆) and N277A (✷) mutations to Dom2 both substantially reduced the ability of yeast bearing these proteins to grow on fluoride. As in Dom1, the insertion of an additional residue in the G*hhh*R motif (▼) results in an $IC_{50}$ value similar to the empty vector (Fig. 10*B*). Unsurprisingly from these results, the double R33A/R255A (◆) and N56A/N277A (✷) mutations rendered Fex1p completely nonfunctional (Fig. 10*C*). Interestingly, the two double mutants G29A/A251G (△) and S97A/S328A (○) had no effect on protein function (Fig. 10*C* and Table 4), suggesting that these highly conserved positions may have a different role than the other residues tested.

Because of their conservation in FEX sequences as well as the results of the alanine mutations, we decided to investigate further the role of the Arg in TM1 and Asn in TM2. To test the role of the positive charge in TM1, we made Arg to Lys and Arg to Glu mutants in Dom1 alone (R33K and R33E), Dom2 alone (R255K and R255E), and both Dom1 and Dom2 (R33K/R255K and R33E/R255E). When the charge of this residue was made negative instead of positive in the Arg to Glu mutant series, protein function was abolished in all but the R33E Dom1 mutant, which retained a modest ability to grow on fluoride. In contrast, when the positive charge was preserved in the Arg to Lys series, even the double R33K/R255K mutant still conferred protection from fluoride toxicity (Fig. 11*A* and Table 4). These results, combined with the data from the Arg to Ala mutants, imply that a positive charge at the end of TM1 is critical, particularly in Dom2.

To interrogate the importance of Asn-56/277 in TM2, we made a series of Asn to Gln mutants (N56Q, N277Q, and N56Q/N277Q), maintaining the amide functional group but extending the side chain by one carbon, and a series of Asn to Asp mutants (N56D, N277D, and N56D/N277D), maintaining the side chain length but replacing the amide with the more polar carboxylic acid moiety. The data demonstrate that lengthening the side chain in either domain is well tolerated, but lengthening it simultaneously in both domains abolishes protein function. When aspartate was substituted, the effects were greater in the single domain mutants (especially for Dom2), and again, the double mutant was nonfunctional (Fig. 11*B* and Table 4).

## Discussion

Fluoride is toxic to yeast at low micromolar levels in the absence of the FEX protein. Here, we provide evidence that FEX is constitutively expressed in *S. cerevisiae*. This situation contrasts not only with that for bacterial Fluc proteins but also with the substrate-regulated expression of both toxic and nontoxic metal ion transporters in yeast (20, 47). Our data do not rule out regulation in response to some other factor such as nutrient availability, growth phase, etc., but the data clearly show expression of FEX in actively growing cells, regardless of the presence of fluoride. This result, combined with the fact that *S. cerevisiae* has retained two functional FEX genes, implies that protection from fluoride toxicity is critical for these organisms.

What could be unique about fluoride relative to other toxic elements yeast may encounter? One possibility is the fact that fluoride can accumulate in living cells because of pH-trapping, which would make even low environmental levels potentially

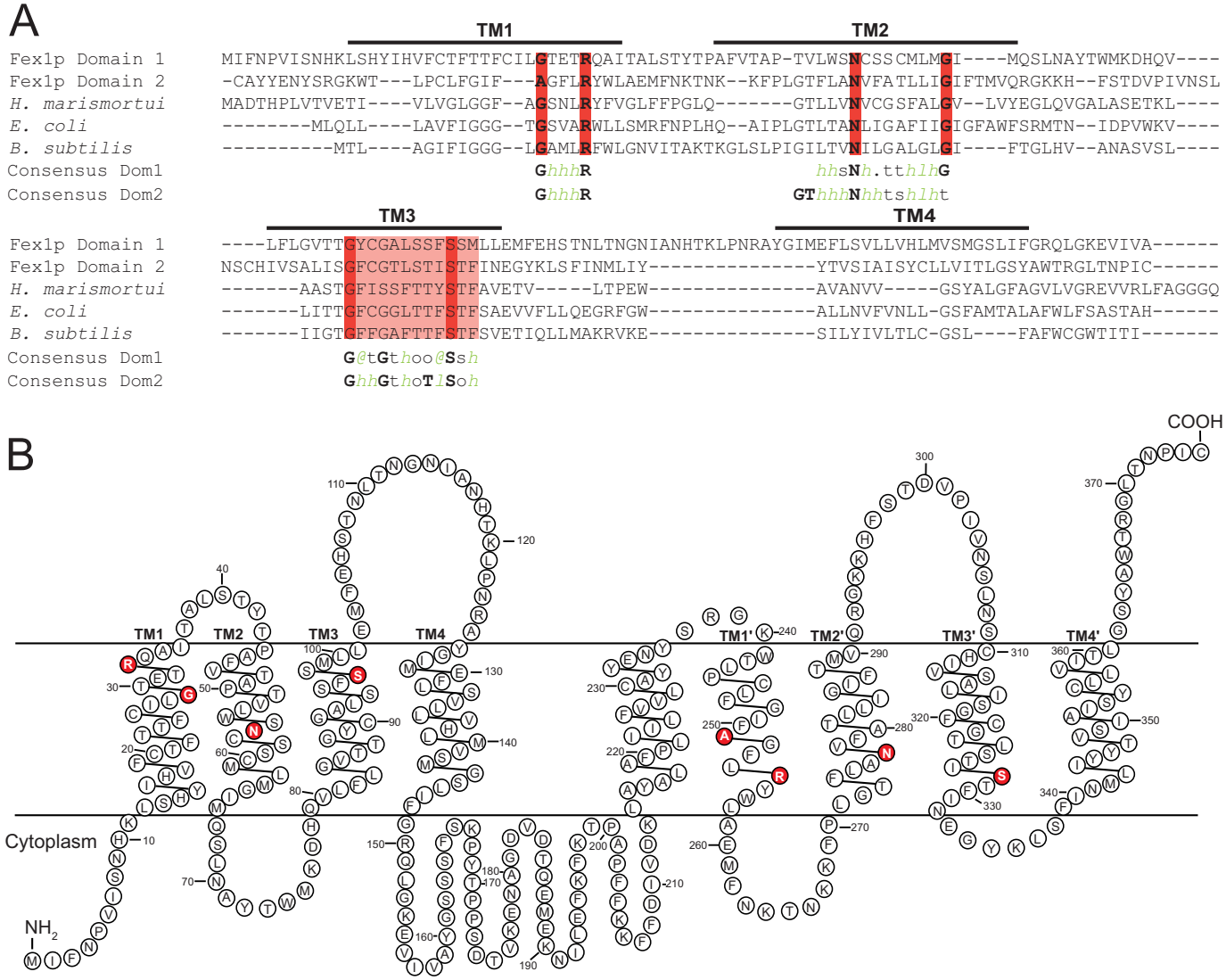


FIGURE 9. **Residue conservation between Fex1p and some of its homologs.** *A,* alignment of Fex1p, one archaeal sequence, and two eubacterial sequences. The eukaryotic consensus sequences for Dom1 and Dom2 as generated by PROMALS3D (46) are shown *below* the alignment. The most conserved amino acids are highlighted in *red*. *h* = hydrophobic (W, F, Y, M, L, I, V, A, C, T, H); *s* = small (A, G, C, S, V, N, D, T, P); *t* = tiny (A, G, C, S); *l* = aliphatic (I, V, L); *@* = aromatic (Y, H, W, F); *o* = alcohol (S, T). *B,* bead diagram of Fex1p, elaborated from the topology model in Fig. 7*A*. Conserved residues targeted for mutagenesis are highlighted in *red*. Boundaries for the TMHs were predicted by TMHMM with the exception of the C-terminal end of TM1. The predicted boundary of this helix does not place Arg-33 within the membrane. However, the conserved nature of this residue, the prediction for Arg-255 in TM1′, and the transmembrane location of the analogous Arg in prokaryotic homologs suggests that Arg-33 likely resides in TM1, and it has been modeled as such.

toxic in the absence of a persistent export mechanism (16, 48). In general, the constitutive expression of ion channels requires that there be some mechanism of regulation to stabilize cellular composition and to conserve metabolic energy. However, the large negative membrane voltage in fungi, −200 to −300 mV (49–51), might confine this practical problem to one of selection, *i.e.* enabling the cells to eject toxic anions but retain metabolically essential anions such as chloride. Indeed, the demonstrated extreme selectivity of Fluc channels for fluoride over chloride (>10,000-fold) should allow these channels to be expressed without deleterious effects from promiscuous transport of other ions, as proposed previously (15). Although we hypothesize that a similar selectivity is utilized by FEX proteins in eukaryotes, it is important for us to develop a more precise assay of FEX channel function in yeast than the whole-cell patch recording presently offers, limiting measured $F^-/Cl^-$ selectivity, thus far, to ~10:1.

Bilayer-reconstituted Fluc from *E. coli* has been unequivocally shown to function as a *bona fide* ion channel, with well defined on-off switching and unit conductances of roughly 10 picosiemens (for solutions containing 300 mM $F^-$) (17). Because eukaryotic FEX proteins conserve critical amino acid residues from their Fluc homologs, the FEX proteins are also expected to behave like ion channels. Although discrete switching events are not visible in the whole-cell records of Figs. 1 and 3, other features of those data are consistent with channel-like behavior, namely the clear relaxation of currents (representing $F^-$ efflux) during maintained voltage steps and the linearizing of current-voltage plots at membrane voltages beyond −150 mV. The quantification of Fex1,2p in *Saccharomyces* plasma

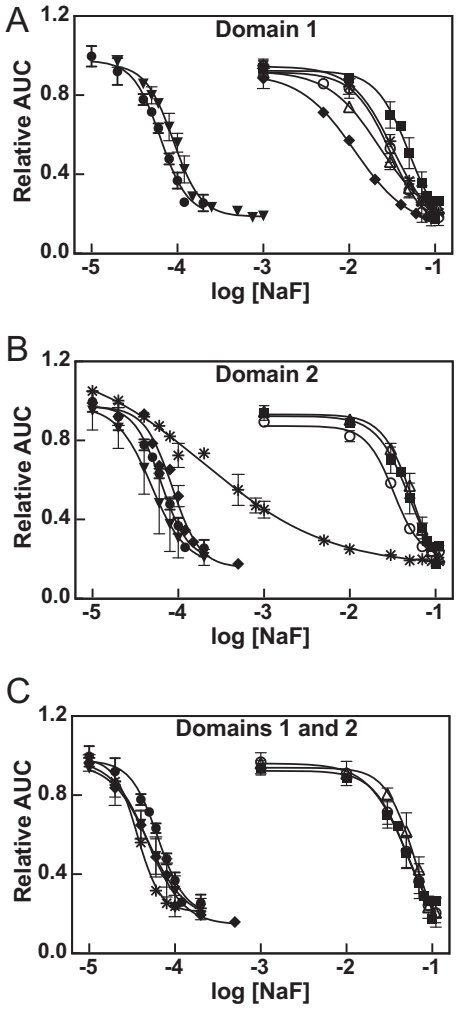


FIGURE 10. **Growth tolerance plots of point mutants of Fex1p.** Relative AUC is the area under the curve normalized to the growth at zero fluoride. The data are fitted to a standard dose-response curve, where each curve was measured a minimum of three times. *Error bars* represent the standard deviation. Wild-type pRS416-*FEX1* (■) and empty pRS416 (●) are shown on each graph for reference. $IC_{50}$ values calculated from these curves are shown in Table 4. *A,* mutations to domain 1: G29A (△), R33A (◆), 32insA (▼), N56A (✳), and S97A (○). *B,* mutations to domain 2: A251G (△), R255A (◆), 254insA (▼), N277A (✳), and S328A (○). *C,* mutations to both domain 1 and 2: G29A/A251G (△), R33A/R255A (◆), 32insA/245insA (▼), N56A/N277A (✳), and S97A/S328A (○).

membranes allows an estimation of the turnover of $\sim 2 \times 10^6$ ions/s for 75 mM $F^-$ in the intracellular solution, consistent with channel behavior. An additional observation consistent with the homologous function of Fluc and FEX proteins is that heterologous expression of Fluc in yeast confers resistance to millimolar concentrations of fluoride.

Despite these functional similarities to Fluc, FEX proteins have an inherent asymmetry in their structure that is absent in many of its bacterial homologs. FEX proteins cannot be fully symmetric both because of sequence dissimilarity between the first four TM helices (Dom1) and the last four (Dom2) and because of topological rigidity imposed by the linker helix (TM5) connecting Dom1 with Dom2 (Fig. 7). Therefore, functional differences between corresponding residues in Dom1 *versus* Dom2 were expected; however, the quantitative extent of those differences was greater than anticipated. Our data clearly show that corresponding mutations to the two domains of FEX have asymmetrical effects on protein function. Specifically, mutations of residues in Dom2 have a much greater effect than those of residues in Dom1.

This kind of asymmetry has already been demonstrated in other proteins composed of inverted repeats. GlpT, for example, is a member of the major facilitator superfamily that transports glycerol 3-phosphate via a 12-TMH structure comprising two 6-TMH halves. The two halves show only a low degree of sequence similarity but fold across a 2-fold axis of symmetry (52). Two related arginines, one in each half of the protein, were first predicted to play symmetric roles in binding the negatively charged substrate, but further work demonstrated that only the Arg in the first half actually contributes to substrate binding (53). Another example comes from the SMR cationic transporter EmrE, which forms an antiparallel dimer similar to FEX (19). When that transporter was mimicked by an artificial dimer with 4 + 1 + 4 topology, the fused protein proved functionally more tolerant of N-domain mutations than of C-domain mutations. Some of this asymmetry is explained by the fact that these fusion proteins appear able to form intermolecular dimers with their C-terminal domains, but at least a fraction form intramolecular dimers analogous to what we expect happens with FEX (54).

Our mutagenesis experiments reveal several residues that seem to be required for fluoride transport. The data imply that either Gly or Ala can be functional in the G*hhh*R motif but that the spacing must be three residues, a result consistent with phylogenetics. It is possible that this Gly is conserved because it is important for helix packing, as is often the case for glycine residues in transmembrane segments (55, 56). Consistent with this, when this residue is mutated to the bulky amino acid Phe, all protein function is lost (Table 4). The G*hhh*R motif is expected to be a part of a TMH, and thus the spacing is likely important to display the Arg side chain in the correct helical register. Interestingly, the Arg is located in a similar position to a conserved glutamate (Glu-14) in EmrE. This SMR protein transports cationic compounds, and the functional form is an antiparallel dimer similar to FEX proteins (19). Glu-14 is located in TM1 of EmrE and is absolutely required for transport of its positively charged cargo (57, 58). We hypothesize that Arg-33/Arg-255 in TM1 of FEX plays a similar role in transport of the negatively charged fluoride ion. Interestingly, arginines are required for transporting anions through other proteins (59, 60). It is possible that the positive charge provided by Arg-33/Arg-255 is part of an electrostatic well for fluoride ions entering the channel.

The Asn-56/Asn-277 in TM2 also appears to be required to form an active fluoride channel. A larger Gln can be tolerated in either Dom1 or Dom2 but not at both positions, indicating that either a steric clash is formed or this residue is partially responsible for defining the size of the ion pore. The fact that Asp is better tolerated than Ala in Dom2 suggests that a polar group is required at this position. Taken together, this series of mutants suggests that the amide group of Asn-56/Asn-277 in TM2 is critical for function and may have a role in creating a correctly sized pore for ion transport.

**TABLE 4**
**$IC_{50}$ values for point mutations of Fex1p**

| TMH | Motif | Mutation | Domain 1 | | Domain 2 | | Domains 1 & 2 | | Symbol in Figure 10 |
|---|---|---|---|---|---|---|---|---|---|
| | | | $IC_{50}$ (mM) | Fold-change | $IC_{50}$ (mM) | Fold-change | $IC_{50}$ (mM) | Fold-change | |
| | | WT[a] | 49 ± 13[b] | 1.0 | 49 ± 13 | 1.0 | 49 ± 13 | 1.0 | ■ |
| | | Vector | 0.066 ± 0.004 | 740 | 0.066 ± 0.004 | 740 | 0.066 ± 0.004 | 740 | ● |
| 1/6 | *G*hhhR | A/G | 24 ± 6 | 2.0 | 54 ± 7 | 0.9 | 60 ± 15 | 0.8 | △ |
| | | F | 0.061 ± 0.009 | 800 | 0.051 ±0.010 | 960 | 0.061 ± 0.015 | 800 | |
| | G*hhhR* | A | 12 ± 2 | 4.1 | 0.091 ± 0.004 | 540 | 0.051 ± 0.005 | 960 | ◆ |
| | | K | 43 ± 13 | 1.1 | 15 ± 2 | 3.3 | 12 ± 1 | 4.1 | |
| | | E | 4.6 ± 0.8 | 11 | 0.13 ± 0.06 | 380 | 0.062 ± 0.008 | 790 | |
| | G*hhh*R | insA | 0.097 ± 0.023 | 510 | 0.053 ± 0.014 | 920 | 0.050 ± 0.008 | 980 | ▼ |
| 2/7 | *N* | A | 32 ± 1 | 1.5 | 0.45 ± 0.22 | 110 | 0.036 ± 0.001 | 1400 | ✳ |
| | | Q | 44 ± 13 | 1.1 | 18 ± 5 | 2.7 | 0.046 ± 0.005 | 1100 | |
| | | D | 32 ± 2 | 1.5 | 5.8 ± 2.7 | 8.5 | 0.067 ± 0.017 | 730 | |
| 3/8 | *S* | A | 29 ± 6 | 1.7 | 33 ± 2 | 1.5 | 49 ± 12 | 1.0 | ○ |

[a] WT is the wild-type *FEX1* gene expressed from pRS416.
[b] All values are the average of at least three trials ± S.D.

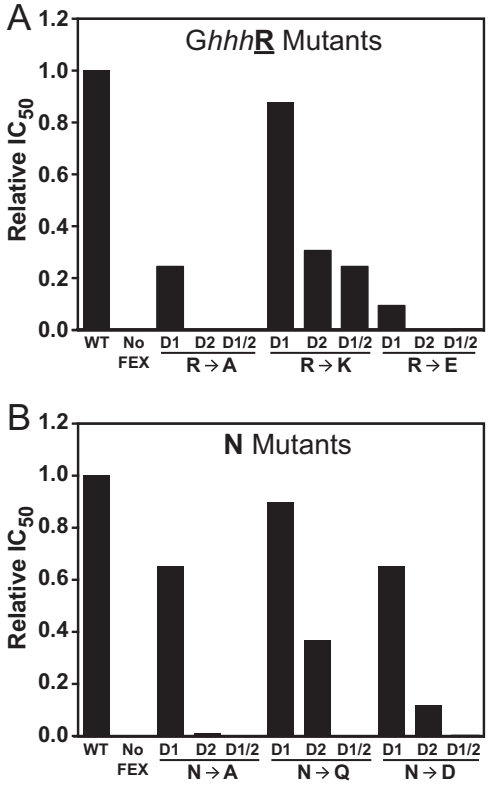


FIGURE 11. **Relative $IC_{50}$ values for mutants of Arg-33 and Arg-255 in TM1 (*A*) and Asn-56 and Asn-277 in TM2 (*B*).** To calculate the relative $IC_{50}$, the point mutant $IC_{50}$ from Table 4 was divided by the $IC_{50}$ value for wild type. *D1* = mutation in domain 1; *D2* = mutation in domain 2; *D1/2* = mutation in both domain 1 and domain 2.

Our mutational analysis also hints at a role in ion selectivity for several residues. Most notable is Ser-97/Ser-328 in TM3 where no effect on the ability of yeast to grow in fluoride was produced by mutation, even when the amino acid in both domains was changed. Additionally, the absolutely conserved Arg-33/Arg-255 in TM1 could be mutated to Lys in both domains with retention of growth on fluoride at near wild-type levels. We hypothesize, then, that these two residues play a role in ion selectivity, rather than in absolute affinity for the substrate. This seems particularly likely in the case of Arg-33/Arg-255, given its positive charge and large size. The fact that Lys can function in its place suggests that the positive charge is necessary for conducting fluoride through the channel, but its absolute conservation as the larger Arg is required to select against larger anions (*e.g.* chloride). Further experiments will be required to fully define the role of these residues in ion selectivity.

The FEX proteins from *S. cerevisiae* are members of a widely distributed family of fluoride selective ion channels. Not only have two functional genes been retained in this species, but both copies are constitutively expressed in *S. cerevisiae*, implying either that these microorganisms are often in contact with fluoride or that the toxic effects of this anion are significant enough to warrant a continuous defense mechanism. In addition to having homologs in many other unicellular organisms (>25,000 bacterial and >300 fungal sequences in Uniprot), homology searches reveal putative FEX proteins in many multicellular organisms, including important crops such as rice, corn, potatoes, apples, grapes, and oranges as well as other industrial plants such as cotton, tobacco, coffee, and cocoa. The presence of FEX homologs in these species suggests that many diverse organisms face the problem of fluoride toxicity and have managed it using a fluoride channel.

*Author Contributions*—K. D. S., A. R., C. S., and S. A. S. designed the study and wrote the paper. K. D. S., P. B. G., A. R., K. E. A., and T. B. performed the experiments and made the figures. All authors analyzed the results and approved the final version of the manuscript.

*Acknowledgments—We thank Mark Hochstrasser, Robert Tomko, Jr., and Jennifer Gillies for the pFA6a-GFP(S65T)-kanMX6, pFA6a-mCherry:natMX4, pRS426, and pRS425 plasmids, pmr1Δ deletion strain, as well as advice and helpful discussions; Gunnar von Heijne and Hyun Kim for the gift of the p424GPD yEGFP E172T HA plasmid; Susan Lindquist for the pAG426GPD-ccdB-HA plasmid; Daniel Spakowicz for help with phylogenetics; and Stanley Thorburn for help with imaging.*

*Note Added in Proof*—During the editing of this manuscript, the crystal structure of the bacterial Fluc protein was determined (Stockbridge, R. B., Kolmakova-Partensky, L., Shane, T., Koide, A., Koide, S., Miller, C., and Newstead, S. (2015) Crystal structures of a dual-topology, double-barreled fluoride ion channel. *Nature*, in press). The structure shows that the bacterial fluoride channel contains two pores, where one pore consists primarily of residues from one subunit and the second pore is made primarily of residues from the second subunit in the dimeric complex. Stockbridge and coworkers hypothesize that in eukaryotic FEX proteins, where the two subunits are fused into a single polypeptide, one pore could be degraded while retaining channel function. This is consistent with our result that mutations of residues in the C-terminal domain are more detrimental to function than the equivalent mutations to the N-terminal domain. It suggests that the channel comprised primarily of the C-terminal domain is the functional element in the yeast FEX protein and the pore from the N-terminal domain has largely lost function.

## References


1. Weinstein, L. H., and Davison, A. W. (2004) *Fluorides in the Environment: Effects on Plants and Animals*, CABI Publishing, Cambridge, MA
2. Jagtap, S., Yenkie, M. K., Labhsetwar, N., and Rayalu, S. (2012) Fluoride in drinking water and defluoridation of water. *Chem. Rev.* **112,** 2454–2466
3. World Health Organization (2006) *Fluoride in Drinking Water*, World Health Organization, Geneva
4. World Health Organization (1970) *Fluorides and Human Health. Switzerland Monograph Series No. 59,* World Health Organization, Geneva
5. World Health Organization (1984) *Fluorine and Fluorides, Environmental Health Criteria 36, IPCS International Programme on Chemical Safety*, World Health Organization, Geneva
6. Smith, F. A., Hodge, H. C., and Dinman, B. D. (1977) Airborne fluorides and man: Part I. *CRC Crit. Rev. Environ. Control.* **8,** 293–371
7. Lesher, R. J., Bender, G. R., and Marquis, R. E. (1977) Bacteriolytic action of fluoride ions. *Antimicrob. Agents Chemother.* **12,** 339–345
8. Baker, J. L., Sudarsan, N., Weinberg, Z., Roth, A., Stockbridge, R. B., and Breaker, R. R. (2012) Widespread genetic switches and toxicity resistance proteins for fluoride. *Science* **335,** 233–235
9. Barbier, O., Arreola-Mendoza, L., and Del Razo, L. M. (2010) Molecular mechanisms of fluoride toxicity. *Chem. Biol. Interact.* **188,** 319–333
10. Lebioda, L., Zhang, E., Lewinski, K., and Brewer, J. M. (1993) Fluoride inhibition of yeast enolase: crystal structure of the enolase-$Mg^{2+}$-$F^-$-Pi complex at 2.6 A resolution. *Proteins* **16,** 219–225
11. Agalakova, N. I., and Gusev, G. P. (2012) Molecular mechanisms of cytotoxicity and apoptosis induced by inorganic fluoride. *ISRN Cell Biol.* **2012,** 1–16
12. Li, L. (2003) The biochemistry and physiology of metallic fluoride: action, mechanism, and implications. *Crit. Rev. Oral Biol. Med.* **14,** 100–114
13. Adamek, E., Pawłowska-Góral, K., and Bober, K. (2005) *In vitro* and *in vivo* effects of fluoride ions on enzyme activity. *Ann. Acad. Med. Stetin.* **51,** 69–85
14. Stockbridge, R. B., Lim, H.-H., Otten, R., Williams, C., Shane, T., Weinberg, Z., and Miller, C. (2012) Fluoride resistance and transport by riboswitch-controlled CLC antiporters. *Proc. Natl. Acad. Sci. U.S.A.* **109,** 15289–15294
15. Stockbridge, R. B., Robertson, J. L., Kolmakova-Partensky, L., and Miller, C. (2013) A family of fluoride-specific ion channels with dual-topology architecture. *eLife* **2,** e01084
16. Li, S., Smith, K. D., Davis, J. H., Gordon, P. B., Breaker, R. R., and Strobel, S. A. (2013) Eukaryotic resistance to fluoride toxicity mediated by a widespread family of fluoride export proteins. *Proc. Natl. Acad. Sci. U.S.A.* **110,** 19018–19023
17. Stockbridge, R. B., Koide, A., Miller, C., and Koide, S. (2014) Proof of dual-topology architecture of Fluc $F^-$ channels with monobody blockers. *Nat. Commun.* **5,** 5120
18. Rapp, M., Granseth, E., Seppälä, S., and von Heijne, G. (2006) Identification and evolution of dual-topology membrane proteins. *Nat. Struct. Mol. Biol.* **13,** 112–116
19. Morrison, E. A., DeKoster, G. T., Dutta, S., Vafabakhsh, R., Clarkson, M. W., Bahl, A., Kern, D., Ha, T., and Henzler-Wildman, K. A. (2012) Antiparallel EmrE exports drugs by exchanging between asymmetric structures. *Nature* **481,** 45–50
20. Wysocki, R., and Tamás, M. J. (2010) How *Saccharomyces cerevisiae* copes with toxic metals and metalloids. *FEMS Microbiol. Rev.* **34,** 925–951
21. Wright, M. B., Howell, E. A., and Gaber, R. F. (1996) Amino acid substitutions in membrane-spanning domains of Hol1, a member of the major facilitator superfamily of transporters, confer nonselective cation uptake in *Saccharomyces cerevisiae*. *J. Bacteriol.* **178,** 7197–7205
22. Dos Santos, S. C., Teixeira, M. C., Dias, P. J., and Sá-Correia, I. (2014) MFS transporters required for multidrug/multixenobiotic (MD/MX) resistance in the model yeast: understanding their physiological function through post-genomic approaches. *Front. Physiol.* **5,** 180
23. Adle, D. J., Sinani, D., Kim, H., and Lee, J. (2007) A cadmium-transporting P1B-type ATPase in yeast *Saccharomyces cerevisiae*. *J. Biol. Chem.* **282,** 947–955
24. Adle, D. J., and Lee, J. (2008) Expressional control of a cadmium-transporting P1B-type ATPase by a metal sensing degradation signal. *J. Biol. Chem.* **283,** 31460–31468
25. Adle, D. J., Wei, W., Smith, N., Bies, J. J., and Lee, J. (2009) Cadmium-mediated rescue from ER-associated degradation induces expression of its exporter. *Proc. Natl. Acad. Sci. U.S.A.* **106,** 10189–10194
26. Sherman, F. (2002) Getting started with yeast. *Methods Enzymol.* **350,** 3–41
27. Kaiser, C., Michaelis, S., Mitchell, A., and Laboratory, C. S. (1994) *Methods in Yeast Genetics: A Cold Spring Harbor Laboratory Course Manual*, Cold Spring Harbor Laboratory Press, Cold Spring Harbor, NY
28. Bertl, A., Bihler, H., Kettner, C., and Slayman, C. L. (1998) Electrophysiology in the eukaryotic model cell *Saccharomyces cerevisiae*. *Pflugers Arch.* **436,** 999–1013
29. Kuroda, T., Bihler, H., Bashi, E., Slayman, C. L., and Rivetta, A. (2004) Chloride channel function in the yeast TRK-potassium transporters. *J. Membr. Biol.* **198,** 177–192
30. Antebi, A., and Fink, G. R. (1992) The yeast $Ca^{(2+)}$-ATPase homologue, PMR1, is required for normal Golgi function and localizes in a novel Golgi-like distribution. *Mol. Biol. Cell* **3,** 633–654
31. Bihler, H., Gaber, R. F., Slayman, C. L., and Bertl, A. (1999) The presumed potassium carrier Trk2p in *Saccharomyces cerevisiae* determines an $H^+$-dependent, $K^+$-independent current. *FEBS Lett.* **447,** 115–120
32. Stefan, C. P., Zhang, N., Sokabe, T., Rivetta, A., Slayman, C. L., Montell, C., and Cunningham, K. W. (2013) Activation of an essential calcium signaling pathway in *Saccharomyces cerevisiae* by Kch1 and Kch2, putative low-affinity potassium transporters. *Eukaryot. Cell* **12,** 204–214
33. Miranda, M., Allen, K. E., Pardo, J. P., and Slayman, C. W. (2001) Stalk segment 5 of the yeast plasma membrane $H^+$-ATPase: mutational evidence for a role in glucose regulation. *J. Biol. Chem.* **276,** 22485–22490
34. Rivetta, A., Allen, K. E., Slayman, C. W., and Slayman, C. L. (2013) Coordination of $K^+$ transporters in neurospora: TRK1 is scarce and constitutive, while HAK1 is abundant and highly regulated. *Eukaryot. Cell* **12,** 684–696
35. Lowry, O. H., Rosebrough, N. J., Farr, A. L., and Randall, R. J. (1951) Protein measurement with the Folin phenol reagent. *J. Biol. Chem.* **193,** 265–275
36. Bähler, J., Wu, J. Q., Longtine, M. S., Shah, N. G., McKenzie, A., 3rd, Steever, A. B., Wach, A., Philippsen, P., and Pringle, J. R. (1998) Heterologous modules for efficient and versatile PCR-based gene targeting in *Schizosaccharomyces pombe*. *Yeast.* **14,** 943–951
37. Gietz, R. D., Schiestl, R. H., Willems, A. R., and Woods, R. A. (1995) Studies on the transformation of intact yeast cells by the LiAc/SS-DNA/PEG procedure. *Yeast* **11,** 355–360
38. Brachmann, C. B., Davies, A., Cost, G. J., Caputo, E., Li, J., Hieter, P., and Boeke, J. D. (1998) Designer deletion strains derived from *Saccharomyces cerevisiae* S288C: a useful set of strains and plasmids for PCR-mediated gene disruption and other applications. *Yeast* **14,** 115–132
39. Christianson, T. W., Sikorski, R. S., Dante, M., Shero, J. H., and Hieter, P.

(1992) Multifunctional yeast high-copy-number shuttle vectors. *Gene* **110,** 119–122
40. Lee, H., Min, J., von Heijne, G., and Kim, H. (2012) Glycosylatable GFP as a compartment-specific membrane topology reporter. *Biochem. Biophys. Res. Commun.* **427,** 780–784
41. Mumberg, D., Müller, R., and Funk, M. (1995) Yeast vectors for the controlled expression of heterologous proteins in different genetic backgrounds. *Gene* **156,** 119–122
42. Barrick, J. E., and Breaker, R. R. (2007) The distributions, mechanisms, and structures of metabolite-binding riboswitches. *Genome Biol.* **8,** R239
43. Heijne, G. (1986) The distribution of positively charged residues in bacterial inner membrane proteins correlates with the trans-membrane topology. *EMBO J.* **5,** 3021–3027
44. Krogh, A., Larsson, B., von Heijne, G., and Sonnhammer, E. L. (2001) Predicting transmembrane protein topology with a hidden Markov model: application to complete genomes. *J. Mol. Biol.* **305,** 567–580
45. Käll, L., Krogh, A., and Sonnhammer, E. L. (2007) Advantages of combined transmembrane topology and signal peptide prediction–the Phobius web server. *Nucleic Acids Res.* **35,** W429–W432
46. Pei, J., Kim, B.-H., and Grishin, N. V. (2008) PROMALS3D: a tool for multiple protein sequence and structure alignments. *Nucleic Acids Res.* **36,** 2295–2300
47. Waldron, K. J., Rutherford, J. C., Ford, D., and Robinson, N. J. (2009) Metalloproteins and metal sensing. *Nature* **460,** 823–830
48. Ji, C., Stockbridge, R. B., and Miller, C. (2014) Bacterial fluoride resistance, Fluc channels, and the weak acid accumulation effect. *J. Gen. Physiol.* **144,** 257–261
49. Blatt, M. R., Rodriguez-Navarro, A., and Slayman, C. L. (1987) Potassium-proton symport in *Neurospora*: kinetic control by pH and membrane potential. *J. Membr. Biol.* **98,** 169–189
50. Kropf, D. L. (1986) Electrophysiological properties of *Achlya* hyphae: ionic currents studied by intracellular potential recording. *J. Cell Biol.* **102,** 1209–1216
51. Madrid, R., Gómez, M. J., Ramos, J., and Rodríguez-Navarro, A. (1998) Ectopic potassium uptake in trk1 trk2 mutants of *Saccharomyces cerevisiae* correlates with a highly hyperpolarized membrane potential. *J. Biol. Chem.* **273,** 14838–14844
52. Huang, Y., Lemieux, M. J., Song, J., Auer, M., and Wang, D.-N. (2003) Structure and mechanism of the glycerol-3-phosphate transporter from *Escherichia coli*. *Science* **301,** 616–620
53. Law, C. J., Enkavi, G., Wang, D.-N., and Tajkhorshid, E. (2009) Structural basis of substrate selectivity in the glycerol-3-phosphate: phosphate antiporter GlpT. *Biophys J.* **97,** 1346–1353
54. Lloris-Garcerá, P., Seppälä, S., Slusky, J. S., Rapp, M., and von Heijne, G. (2014) Why have small multidrug resistance proteins not evolved into fused, internally duplicated structures? *J. Mol. Biol.* **426,** 2246–2254
55. Javadpour, M. M., Eilers, M., Groesbeek, M., and Smith, S. O. (1999) Helix packing in polytopic membrane proteins: role of glycine in transmembrane helix association. *Biophys. J.* **77,** 1609–1618
56. Ubarretxena-Belandia, I., and Engelman, D. M. (2001) Helical membrane proteins: diversity of functions in the context of simple architecture. *Curr. Opin. Struct. Biol.* **11,** 370–376
57. Muth, T. R., and Schuldiner, S. (2000) A membrane-embedded glutamate is required for ligand binding to the multidrug transporter EmrE. *EMBO J.* **19,** 234–240
58. Yerushalmi, H., and Schuldiner, S. (2000) An essential glutamyl residue in EmrE, a multidrug antiporter from *Escherichia coli*. *J. Biol. Chem.* **275,** 5264–5269
59. Modi, N., Bárcena-Uribarri, I., Bains, M., Benz, R., Hancock, R. E., and Kleinekathöfer, U. (2013) Role of the central arginine R133 toward the ion selectivity of the phosphate specific channel OprP: effects of charge and solvation. *Biochemistry* **52,** 5522–5532
60. Yang, T., Liu, Q., Kloss, B., Bruni, R., Kalathur, R. C., Guo, Y., Kloppmann, E., Rost, B., Colecraft, H. M., and Hendrickson, W. A. (2014) Structure and selectivity in bestrophin ion channels. *Science* **346,** 355–359

# Yeast Fex1p Is a Constitutively Expressed Fluoride Channel with Functional Asymmetry of Its Two Homologous Domains

Kathryn D. Smith, Patricia B. Gordon, Alberto Rivetta, Kenneth E. Allen, Tetyana Berbasova, Clifford Slayman and Scott A. Strobel

*J. Biol. Chem. 2015, 290:19874-19887.*
*doi: 10.1074/jbc.M115.651976 originally published online June 8, 2015*